DOI: 10.17725/rensit.2019.11.315

Conduction mechanism of nanographite formed by methane plasma deposition and subsequently heat treatment

Efim P. Neustroev, Aisen R. Prokopiev

Ammosov North-Eastern Federal University, https://www.s-vfu.ru
Yakutsk 677000, Russian Federation

E-mail: neustr@mail.ru, aisenprokopiev@mail.ru

Received *01.11.2019, peer reviewed 11.11.2019, accepted 18.11.2019*

Abstract. **Samples of nanographite films obtained by carbon deposition in a methane plasma and subsequent heat treatment at a temperature of 650°C were studied. Thickness of obtained films was 1-2 nm. The results of measurements of a temperature dependencys of the resistance (R(T)) shows that when a temperature changes from 80°K to 300°K the resistance changes by about three orders of magnitude. The temperature dependency of the activation energy has a non-Arrhenius character corresponding to the variable range hopping mechanism. An analysis of the dependency of the reduced activation energy versus the natural logarithm of temperature showed that the electric conductivity of graphite nanoflakes corresponds to the Efros-Shklovsky mechanism. Size of graphite nanoflakes was estimated to be ~1.7 nm from the obtained results.**

Keywords: **plasma-enhanced deposition, methane, heat treatment, nanographite, electrical conductivity**

PACS: 73.25.+i, 73.50.Mx, 73.61.-r.

Acknowledgements: This work was carried out within the framework of projects of the Ministry of Science and Higher Education of the Russian Federation (project FSRG-2017-0017) and a grant from the Russian Science Foundation (project 19-32-90133 Postgraduate students).

*For citation***:** Efim P. Neustroev, Aisen R. Prokopiev. Conduction mechanism of nanographite formed by methane plasma deposition and subsequently heat treatment. *RENSIT*, 2019, 11(3):315-320; DOI: 10.17725/rensit.2019.11.315.

Contents

1. INTRODUCTION

Nanographite can serve as a precursor for producing graphene [1]. Graphene and its derivatives are of interest not only because of their high electrical and thermal conductivity as well as mechanical strength [2, 3], but also due to their sensory properties for

creation of optoelectronic, biological, gas and mechanical sensors [2, 4] and wide possibilities for practical application. The most popular methods for producing graphene are Chemical Vapor Deposition (CVD) [5] and its modification – plasma-enhanced chemical vapor deposition (PECVD) [5]. As a rule, PECVD method uses hydrocarbons (CH_4 or C_2H_2) as sources of carbon [6, 7]. PECVD method possesses numerous advantages including the possibility of temperature drop to 450°*C* without using catalysts [6] and increase in the deposition rate [6] during the process. At the same time, direct plasma exposure can lead to the formation of a high density of defects [8] in the films formed and the formation of vertical carbon structures due to the intrinsic electric field [5]. The formation of defects and vertical growth can be reduced by the remote plasma-enhanced chemical deposition method, in which the reaction chambers of the plasma system and the CVD devices are spatially separated while the gas flows are combined [9]. On the other hand, such method complicates the installation for producing graphene and increases its cost. This study used the method of separate use of plasma deposition and heat treatment in the form of two independent sequential stages. The electrical and structural properties of the obtained material were investigated.

2. MATERIALS AND METHODS

First stage of obtaining the samples involved deposition of carbon on the surface of SiO_2 in a CH_4 methane plasma at temperatures that were close to ambient. The power of the generated inductively coupled plasma (13.56 MHz) ranged from 150 to 200W. The reaction was carried out in a chamber previously evacuated to pressure of 0.001 mbar. When methane was launched at a flow rate of 30cm^3/min, the operating pressure in the chamber rose to 0.03 mbar. Total time of processing samples in plasma was up to 12 min. At the second stage, the samples were subjected to heat treatment at a temperature 650°*C* for 30 min in an argon atmosphere. The obtained carbon films were studied by Raman spectroscopy (Ntegra Spectra), Atomic Force Microscopy (AFM) (Ntegra Spectra), and temperature dependencies of the resistances, measured in the range from 80° K to 300° K using a two-probe method.

3. RESULTS

Fig. 1*a* shows the Raman spectra of a sample treated in CH_4 plasma with a power of P = 200 W for 12 min before and after annealing. A wide photoluminescence band observed after plasma exposure is typical for hydrogenated amorphous carbon film (a-C:H) [10]. After heat treatment, this

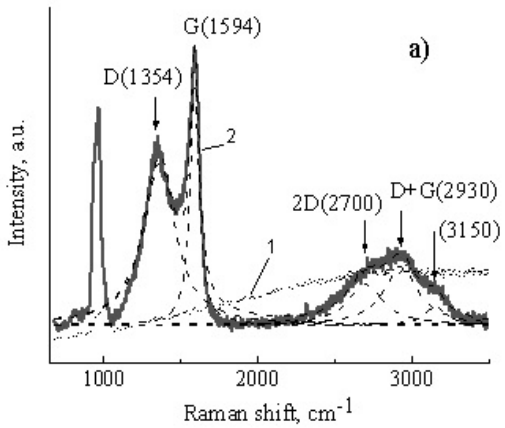

Fig. 1*a. Raman spectra of the sample: 1 - after processing in plasma (P = 200 W, 12 min), 2 - after annealing.*

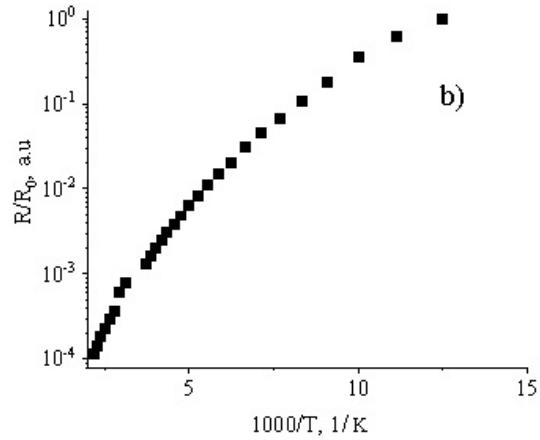

Fig. 1*b. The dependency of the value of relative resistance on the return temperature.*

band practically disappears. D-, G-peaks and their overtones (2D, D+G) corresponding for nanocrystalline graphite structures appear [11]. The nature of the peak at the ~3150cm^{-1} connects with vibrations of the carbon-hydrogen bonds of the aromatic carbon ring [11]. The band observed in the range from 920cm^{-1} to 1050cm^{-1} is connected with the SiO_2 substrate [12]. An increase in its intensity after heat treatment can be explained by a decrease in the thickness of the deposited amorphous film, which was confirmed by the results of AFM measurements.

Fig. 1*b* shows the $R(T)$-dependency normalized relatively to resistance at a temperature of 80° K. At the temperature less than 300° K, $R(T)$ has a nonlinear character and changes by more than three orders of magnitude with a decrease temperature to 80° K. In this case, it can be described by following equation [13]:

$$R(T) = R_0 \exp\left(\frac{T_0}{T}\right)^n, \quad (1)$$

where R_0 is a constant coefficient and T_0 is a characteristic temperature.

The exponent depends on the mechanism of conductivity and takes values of 1⁄2, 1⁄3 or 1⁄4 depending on the model of transfer of charge carrier. Values n = 1⁄2, 1⁄3 and 1⁄4 correspond to variable range hopping mechanisms in accordance with the Efros-Shklovsky model, for $2D$ and $3D$ systems, respectively [13, 14]. Value n can be determined from the dependency of LnR on T^{-n} although graphs for n shown on Fig. 1*b* are equal to 1⁄2, and 1⁄3 do not allow to determine exactly which of them more accurately describes the experimental data. Therefore, the self-consistent method was used to refine the value of n [13]. Such method allows to determine $lnW = A - n \times lnT$ using

the equation, where W is the reduced activation energy determined from the following expression:

$$W = -\frac{\partial \ln R(T)}{\partial T} = n\left(\frac{T_0}{T}\right)^n. \quad (2)$$

Fig. 1*c* shows the dependency of lnW on lnT from the slope to which a value of $n = 1/2$ was found which corresponds to the law of Efros-Shklovsky. A slight deviation with increasing temperature can be caused by the influence of the thermo-activation mechanism prevailing at the T less than 300° K.

For the Efros-Shklovsky model, the characteristic temperature T_0 is determined by the following expression [13]:

$$T_o = T_{ES} = \frac{2.8e^2}{4\pi\varepsilon\varepsilon_0 k_B \xi}, \quad (3)$$

where e is the electron charge, ε_0 is the electric constant, ε is the relative permittivity, and ξ is the length of the range of localization of the electron wave function that corresponds to the

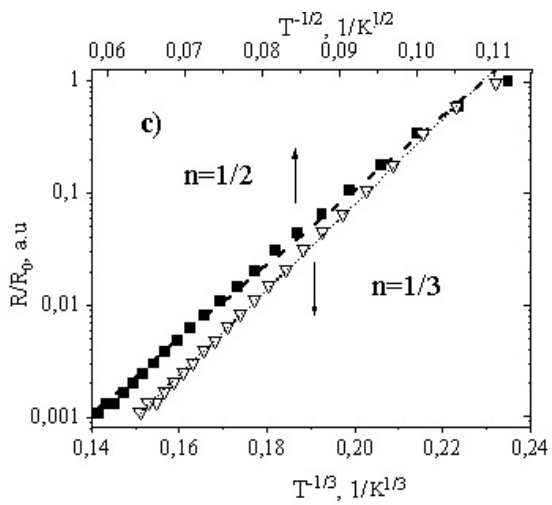

Fig. 1*c. Dependencies of relative resistances on $T^{-1/2}$ and $T^{-1/3}$.*

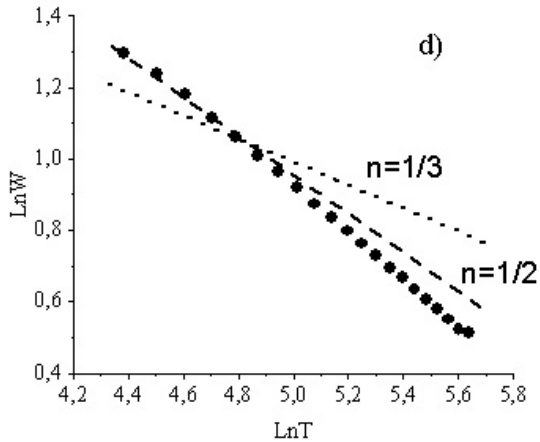

Fig. 1*d. Graph of the reduced activation energy versus the temperature on a logarithmic scale.*

half-length of the graphene domain. The value of the characteristic temperature T_0 was determined from the slope of the lnR dependency on $T^{-1/2}$ (Fig. 1c) which was ~13500° K. From the AFM measurements, the thickness of the investigated film and the number of layers L = 3-4 were determined (with a graphene layer thickness of 3.41 Å). Taking ε = 4 for graphene flakes with the number of layers L [15], a value of = 0.85 nm was found from (3). Thus, a size of the graphene domain equal to $d = 2$ =~ 1.7 nm in nanocrystalline graphite.

4. CONCLUSION

The properties of carbon films formed as a result of plasma treatment in methane and subsequent annealing at $T = 650°C$ were studied. Peaks typical for nanocrystalline graphite are observed in the Raman spectra of the samples obtained. Mechanism of electrical conductivity was

established out of $R(T)$ dependency corresponding to the Efros-Shklovsky law for localized states in graphene domains. Based on this, the size of graphite nanocrystallites was estimated and the value of ~1.7 nm was obtained.

Acknowledgments

The reported study was funded by Ministry of Science and Higher Education of the Russian Federation (project FSRG-2017-0017) and RFBR project number 19-32-90133.

REFERENCES

1. Çelik Y, Flahaut E, Suvacı E. A comparative study on few-layer graphene production by exfoliation of different starting materials in a low boiling point solvent. *FlatChem.*, 2017, 1:74-88.
2. Novoselov KS, Fal'ko VI, Colombo L, Gellert PR, Schwab MG, Kim K. A roadmap for graphene. *Nature*, 2012, 490(7419):192.
3. Papageorgiou DG, Kinloch IA, Young RJ. Mechanical properties of graphene and graphene-based nanocomposites. *Progress in Materials Science*, 2017, 90:75-127.
4. Chen D, Feng H, Li J. Graphene oxide: preparation, functionalization, and electrochemical applications. *Chemical reviews*, 2012, 112(11):6027-6053.
5. Tan H, Wang D, Guo Y. Thermal growth of graphene: A review. *Coatings,* 2018, 8(1):40.
6. Azam MA, Zulkapli NN, Dorah N, Seman R-A, Ani M, Sirat M, Ismail E, Fauzi F, Mohamed M, Majlis B. Critical considerations of high quality graphene synthesized by plasma-enhanced chemical vapor deposition for electronic and energy storage devices. *ECS Journal of Solid State Science and Technology*, 2017, 6(6):M3035-M3048.
7. Khan A, Islam SM, Ahmed S. Direct CVD Growth of Graphene on Technologically Important Dielectric and Semiconducting Substrates. *Advanced Science*, 2018, 5(11):1800050.
8. Neustroev EP, Burtseva EK, Soloviev BD, Prokopiev AR, Popov VI, Timofeev VB. Modification of graphene oxide films by radiofrequency N_2 plasma. *Nanotechnology*, 2018, 29(14):144002.
9. Cuxart MG, Šics I, Goñi AR, Pach E, Sauthier G, Paradinas M, Foerster M, Aballe L, Moreno Fernandez H, Carlino V, Pellegrin E. Inductively coupled remote plasma-enhanced chemical vapor deposition (rPE-CVD) as a versatile route for the deposition of graphene micro- and nanostructures. *Carbon*, 2017, 117:331-342.
10. Ferrari AC, Robertson J. Interpretation of Raman spectra of disordered and amorphous carbon.

Physical review B, 2000, 61(20):14095.

11. Beams R, Cançado LG, Novotny L. Raman characterization of defects and dopants in graphene. *Journal of Physics: Condensed Matter,* 2015, 27(8):P.083002.
12. Uchinokura K, Sekine T, Matsuura E. Raman scattering by silicon. *Solid State Communications,* 1972, 11(1):47-49.
13. Joung D, Khondaker SI. Efros-Shklovskii variable-range hopping in reduced graphene oxide sheets of varying carbon sp^2 fraction. *Physical Review B*, 2012, 86(23):235423.
14. Muchharla B, Narayanan TN, Balakrishnan K.. Temperature dependent electrical transport of disordered reduced graphene oxide. *2D Materials,* 2014, 1(1):011008.
15. Santos EJG. Electric field effects on graphene materials. *Exotic Properties of Carbon Nanomatter*. Springer, Dordrecht, 2015, p. 383-391.